Supporting Information for:

Bilayer Quantum Hall States in an n-type Wide Tellurium Quantum Wells

Chang Niu[1,2], Gang Qiu[1,2], Yixiu Wang[3], Mengwei Si[1,2], Wenzhuo Wu[3] and Peide D. Ye[1,2,*]

[1]*School of Electrical and Computer Engineering, Purdue University, West Lafayette, IN 47907, United States*

[2]*Birck Nanotechnology Center, Purdue University, West Lafayette, IN 47907, United States*

[3]*School of Industrial Engineering, Purdue University, West Lafayette, IN 47907, United States*

* Address correspondence to: yep@purdue.edu (P.D.Y.)

1. Original and second derivative Landau level mapping

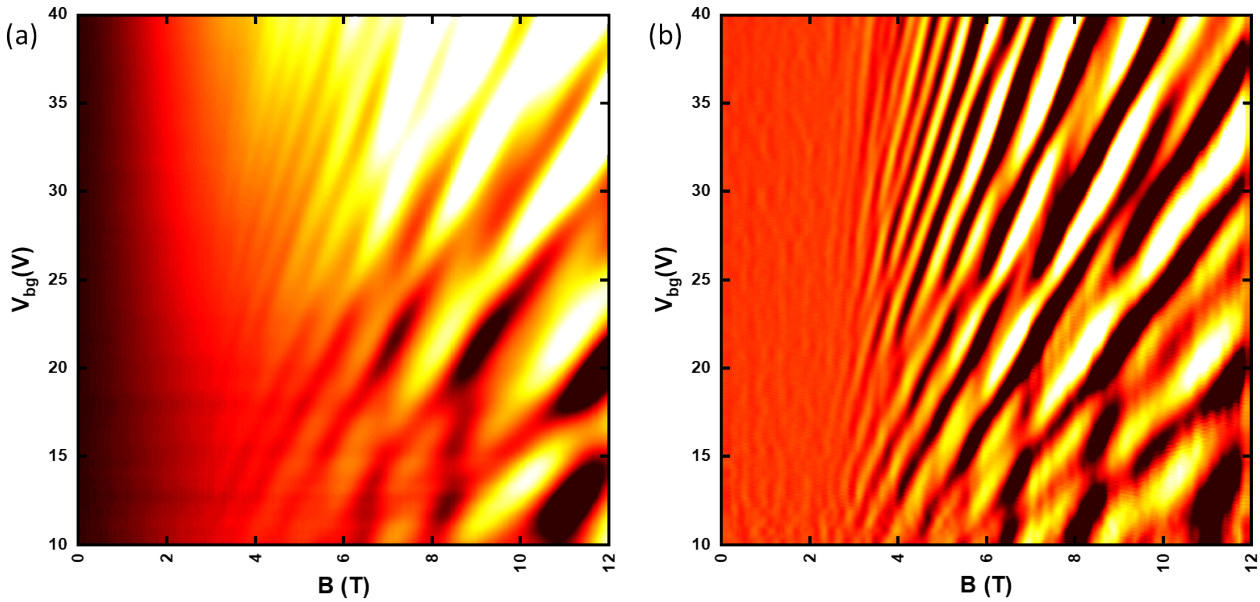

Figure S1 Back gate voltage and magnetic field mapping of longitudinal resistance at 5K and V_{tg}=0V. The bright areas are resistance maxima which are crossing points formed by top and bottom layer Landau levels. (a) Original data (R_{xx}) mapping. (b) The second derivative of R_{xx} with respect to B field ($-\partial^2 R_{xx}/\partial B^2$) mapping shows the same information with more clarity compared to original data (R_{xx}).

2. Landau level hybridization between top and bottom layer 2DEGs

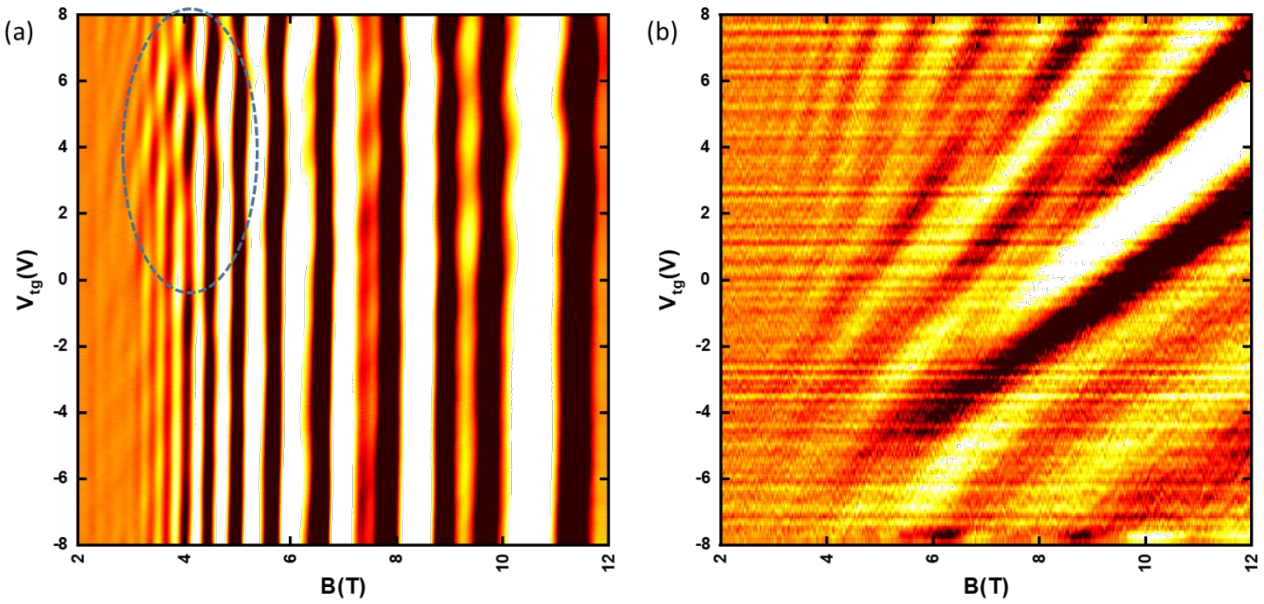

Figure S2 (a) Top gate and magnetic field mapping of the second derivative of R_{xx} with respect to magnetic field ($-\partial^2 R_{xx}/\partial B^2$). (b) Top gate and magnetic field mapping of the second derivative of R_{xx} with respect to top gate voltage ($-\partial^2 R_{xx}/\partial V_{tg}^2$). The bottom layer Landau level distortion (circled in blue) can be explained by the interaction between top layer and bottom layer.

Figure S2(a) and (b) shows the quantum oscillation of Landau levels from bottom and top layer 2DEGs respectively. Landau level crossing features are clearly seen in the blue circle area. By comparing the Landau level sequences between top and bottom layer we can conclude that the crossing features are originated from the interaction between quantum oscillations.

3. Magnetic field B dependence of bilayer quantum oscillations

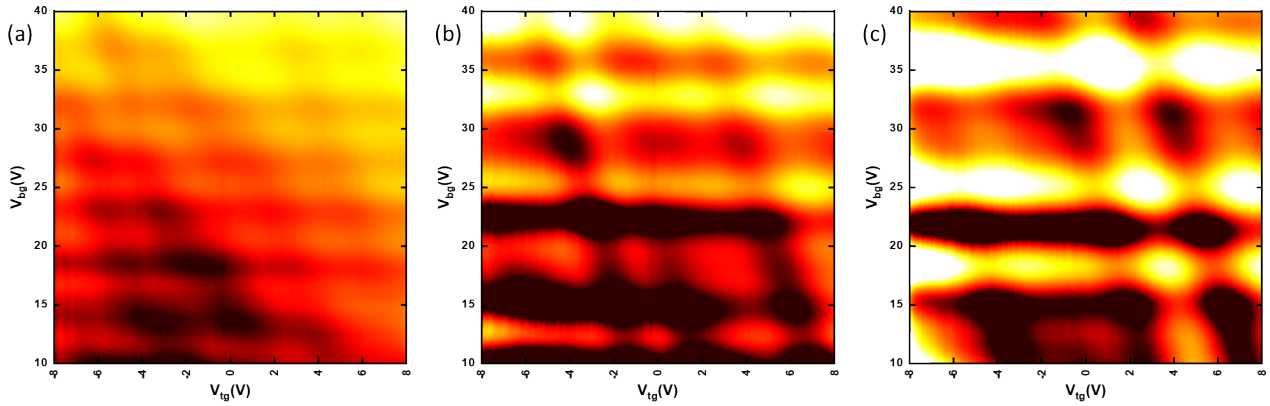

Figure S3: Top gate voltage and back gate voltage mapping of Rxx at different magnetic field: (a) 6T (b) 9T (c) 12T. The temperature is 8K.

4. Top gate dependence of bottom layer Landau level mapping

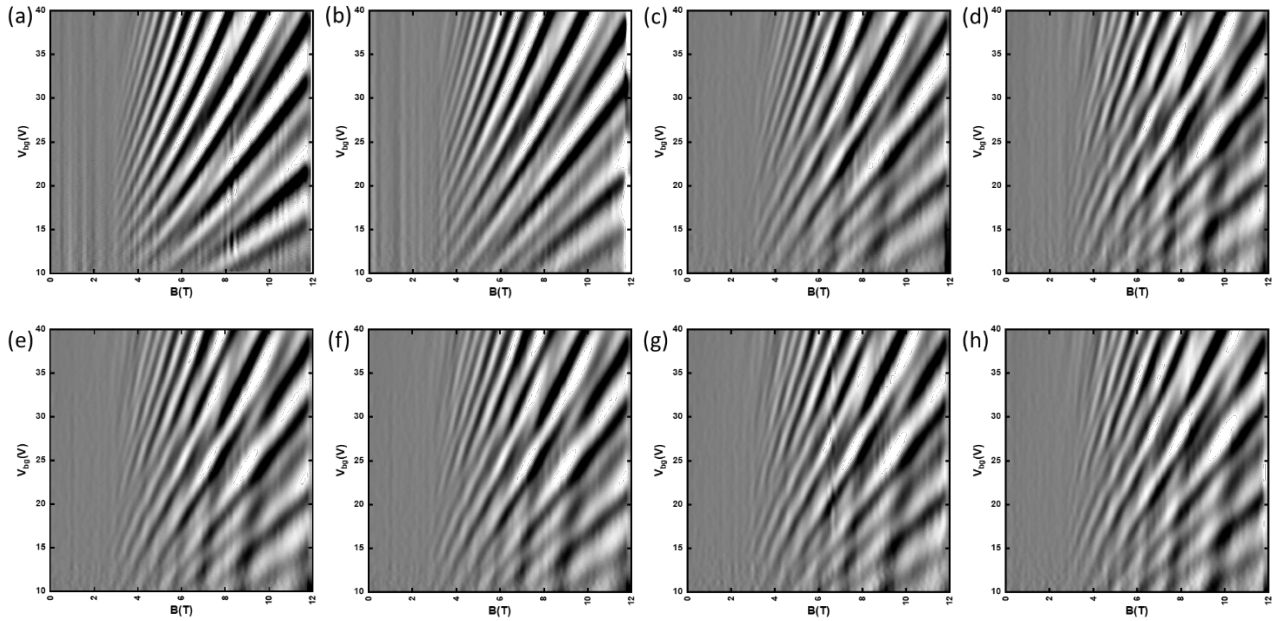

Figure S4: (a)-(h) Back gate and magnetic field mapping of the second derivative of R_{xx} with respect to B field ($-\partial^2 R_{xx}/\partial B^2$) at different top gate voltage, ranging from -8V to 6V with 2V step size. The temperature is 8K.

Quantum oscillations from top layer 2DEG gradually appears with increasing oscillation frequency from V_{tg} = -8 V to V_{tg} = 6 V.

5. Back gate dependence of top layer Landau levels

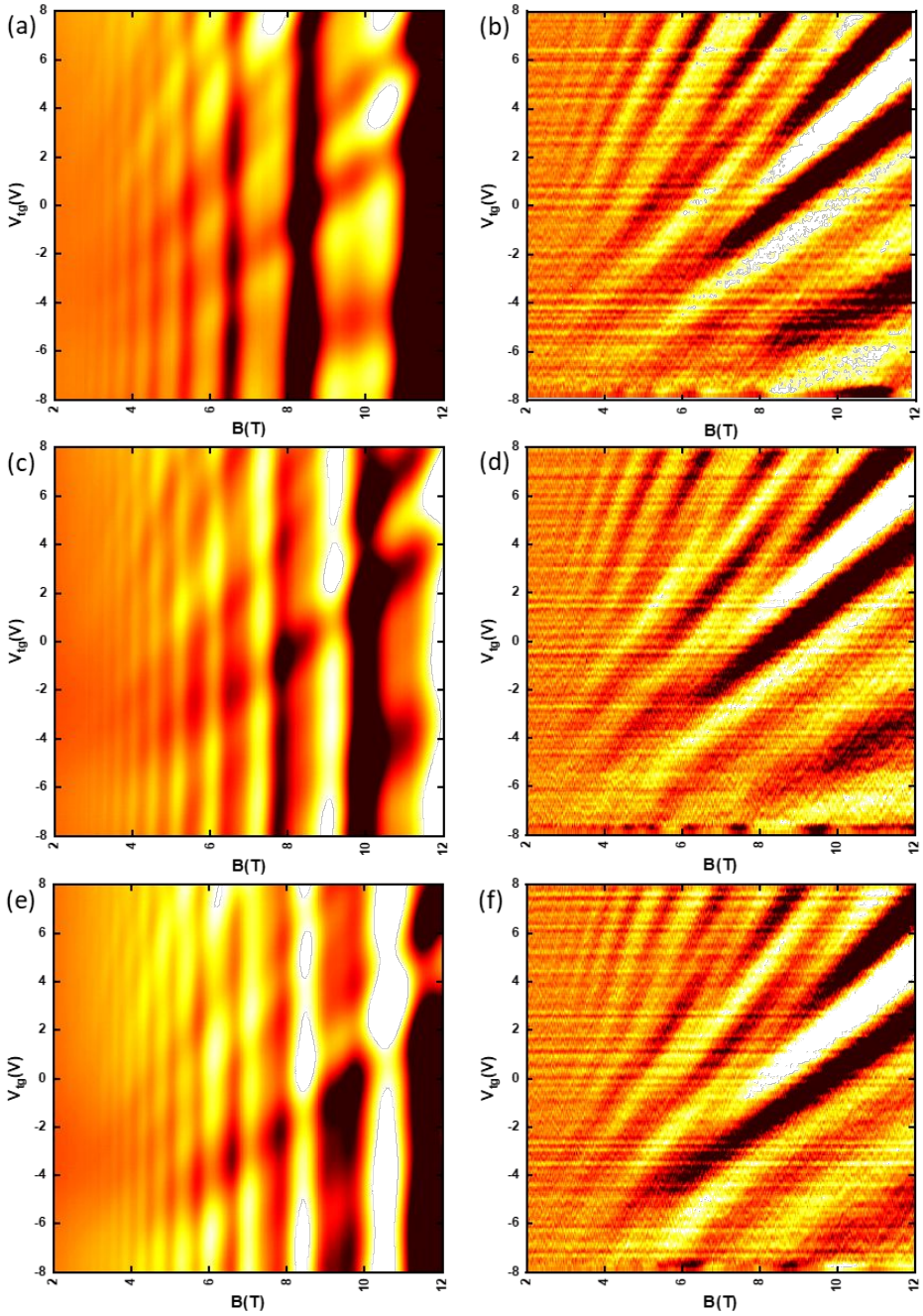

Figure S5 Top gate voltage and magnetic field mapping of R_{xx} at different back gate voltage, (a) 20V (c) 25V (d) 30V. Top gate voltage and magnetic field mapping of the second derivative of R_{xx} with respect to top gate voltage ($-\partial^2 R_{xx}/\partial V_{tg}^2$) at different back gate voltage, (b) 20V (d) 25V (f) 30V. The temperature is 3K.

6. Total carrier density calculated from Hall measurement

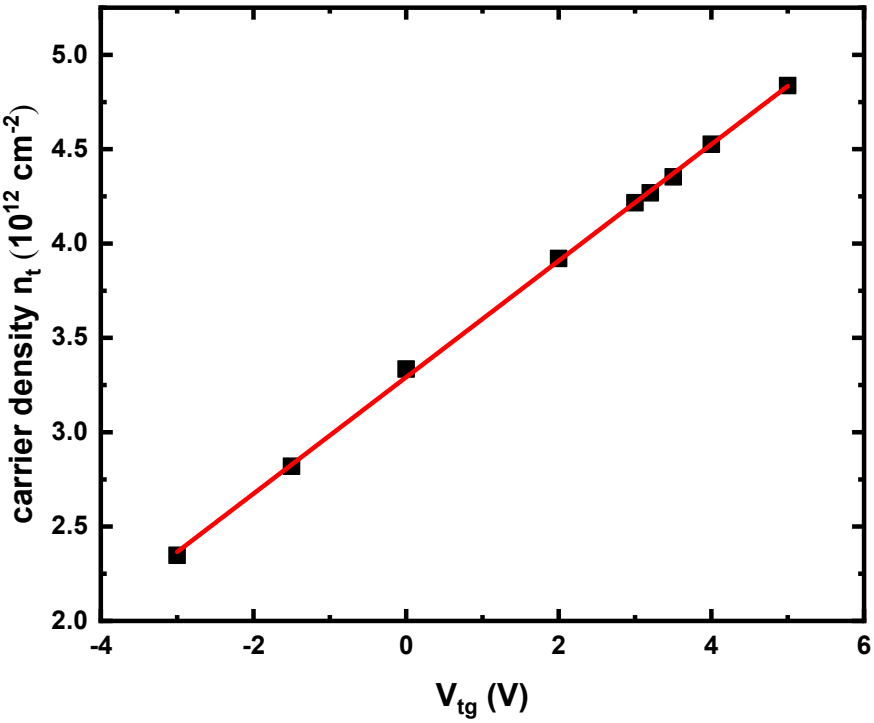

Figure S6 Total electron density (top and bottom layer) calculated from Hall data

The carrier density of the double gated Te FET at fixed V_{bg} = 10 V is calculated from Hall measurement at different V_{tg}. We use the Hall data under 5 T to avoid the influence of quantum Hall effect.

7. Charge transferable states at higher filling factors

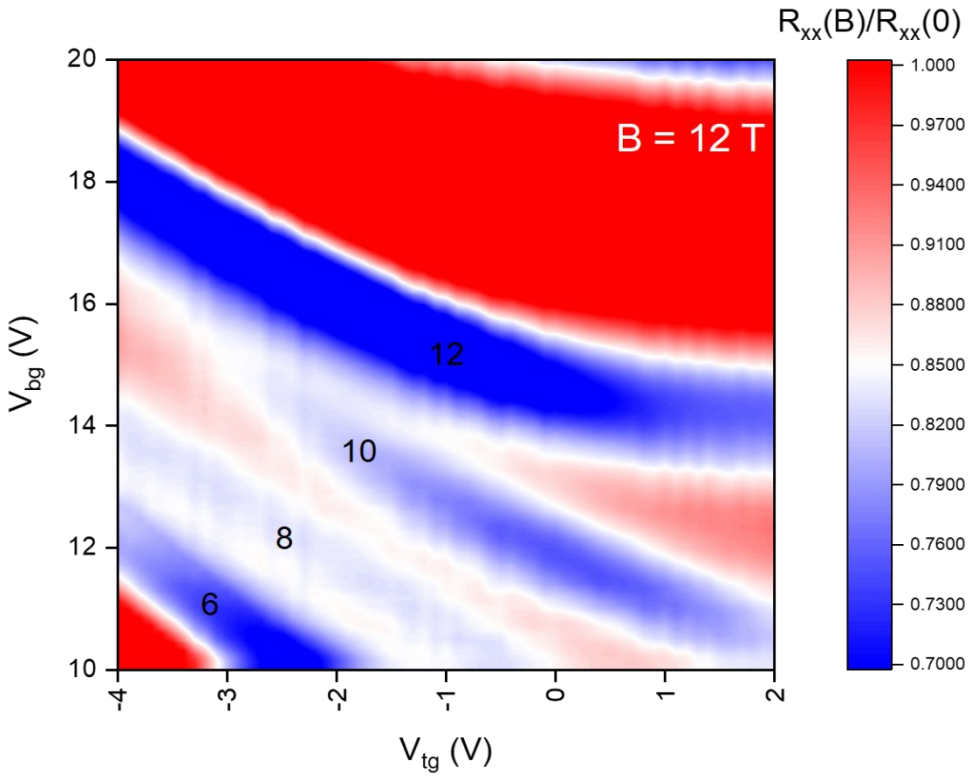

Figure S7 Color mapping of R_{xx} by changing both top and back gate voltage at the magnetic field of 12 T. The Landau levels (filling factor 6, 8, 10 and 12) are controlled by both top and back gate voltage.

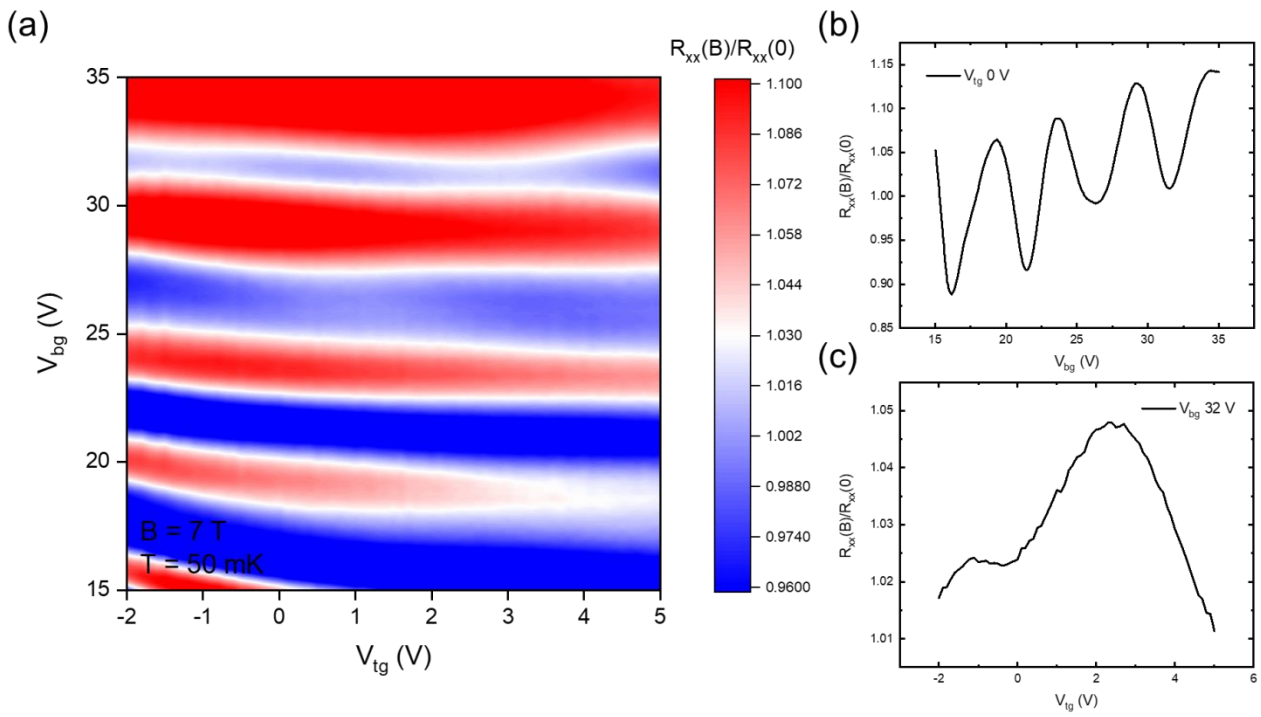

Figure S8 (a) Color mapping of R_{xx} by changing both top and back gate voltage at the magnetic field of 7 T. (b) Bottom layer quantum oscillation at V_{tg} = 0 V. (c) Top layer quantum oscillation at V_{bg} = 32 V.

Figure S7 shows the color mapping of R_{xx} in another similar double-gated 2D Te device with the thickness around 20 nm. The continues quantum Hall states of filling factor 6, 8, 10 and 12 indicate the charge transferable states in 2D Te wide quantum wells. Figure S8 show the quantum oscillations at the magnetic field of 7 T. Two sets of quantum oscillations originated from top and bottom layer 2DEG are identified.

8. Topological non-trivial π Berry phase in quantum Hall sequences in both top and bottom layer electrons.

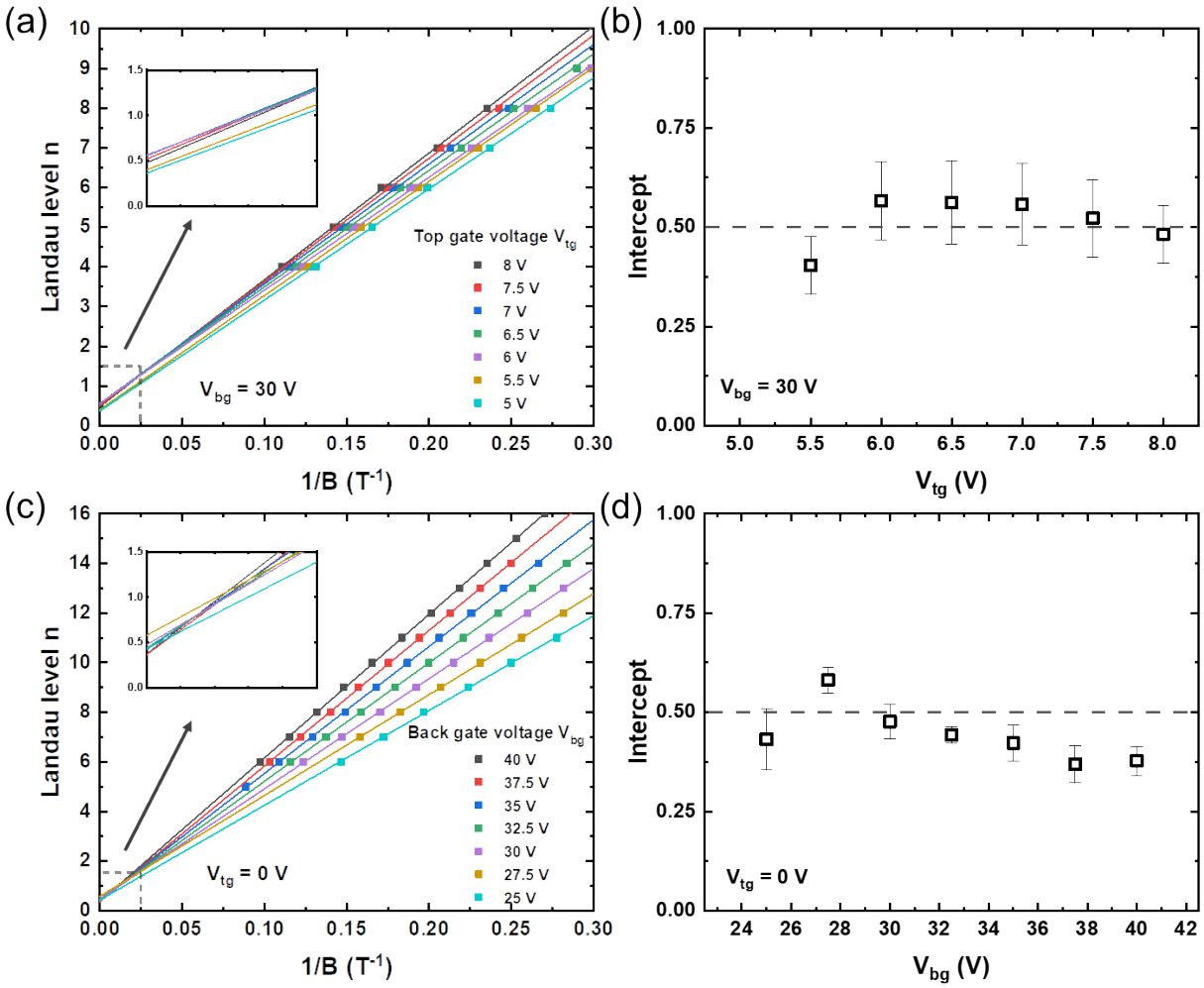

Figure S9 (a) Landau fan diagram under different top gate voltages V_{tg}. The back gate voltage is fixed at 30 V. Inset: magnified view of grey dashed box in (a) with linear fittings extrapolated to the y axis. (b) Intercept of linear fitting versus top gate voltages. The grey dashed line corresponds to the π Berry phase. (c) Landau fan diagram under different back gate voltages V_{bg}. (d) Intercept of linear fitting versus back gate voltages. The minima in quantum oscillations are assigned to integer Landau level n.

The top layer quantum oscillations can be extracted from the mapping of the R_{xx} by sweeping both the magnetic field B and the top gate voltage V_{tg}. The threefold screw symmetry of the Tellurium crystal protected the Weyl node at the edge of the conduction band[1,2]. Because of the Weyl node at H point, the cyclotron picks up a π Berry phase in the quantum Hall sequences.

In Figure S9, we extracted the quantum oscillations from both top and bottom layer 2DEG. We assigned the integer Landau level n to the minima of the quantum oscillations. The 0.5 intercept in Landau fan diagram (top layer Figure S9(a and b), back layer Figure S9(c and d)) indicates the π Berry phase caused by the Weyl fermions.

References

(1) Qiu, G.; Niu, C.; Wang, Y.; Si, M.; Zhang, Z.; Wu, W.; Ye, P. D. Quantum Hall Effect of Weyl Fermions in N-Type Semiconducting Tellurene. *Nat. Nanotechnol.* **2020**, *15* (7), 585–591.

(2) Hirayama, M.; Okugawa, R.; Ishibashi, S.; Murakami, S.; Miyake, T. Weyl Node and Spin Texture in Trigonal Tellurium and Selenium. *Phys. Rev. Lett.* **2015**, *114* (20), 206401.